THE JOURNAL OF BIOLOGICAL CHEMISTRY VOL. 287, NO. 19, pp. 15837–15850, May 4, 2012

Evolutionarily Conserved Paired Immunoglobulin-like Receptor α (PILRα) Domain Mediates Its Interaction with Diverse Sialylated Ligands[S]

Received for publication, July 26, 2011, and in revised form, February 28, 2012 Published, JBC Papers in Press, March 6, 2012, DOI 10.1074/jbc.M111.286633

Yonglian Sun[‡], Kate Senger[‡], Tomasz K. Baginski[§], Anita Mazloom[¶], Yvonne Chinn[¶], Homer Pantua[‖], Kajal Hamidzadeh[‡], Sree Ranjani Ramani[¶], Elizabeth Luis[¶], Irene Tom[¶], Andrew Sebrell[**], Gabriel Quinones[¶], Yan Ma[‡‡], Kiran Mukhyala[‡‡], Tao Sai[**], Jiabing Ding[‡], Benjamin Haley[¶], Hooman Shadnia[§§], Sharookh B. Kapadia[‖], Lino C. Gonzalez[¶], Philip E. Hass[¶], and Ali A. Zarrin[‡1]

*From the Departments of [‡]Immunology, [§]Protein Analytical Chemistry, [¶]Protein Chemistry, [‖]Microbial Pathogenesis, **Antibody Engineering, and [‡‡]Bioinformatics and Computational Biology, Genentech, South San Francisco, California 94080 and the [§§]Chemical Computing Group Inc., Montreal H3A2R7, Quebec, Canada*

Background: PILRα is an inhibitory receptor predominantly expressed in myeloid cells.
Results: NPDC1 and COLEC12 are novel PILRα ligands. PILRα arginine residues 133 (mouse) and 126 (human) are critical contact residues.
Conclusion: PILRα/ligand interactions involve a conserved domain in PILRα and a sialylated protein domain in the ligand.
Significance: PILRα interacts with various ligands to alter myeloid cell function.

Paired immunoglobulin-like receptor (PILR) α is an inhibitory receptor that recognizes several ligands, including mouse CD99, PILR-associating neural protein, and Herpes simplex virus-1 glycoprotein B. The physiological function(s) of interactions between PILRα and its cellular ligands are not well understood, as are the molecular determinants of PILRα/ligand interactions. To address these uncertainties, we sought to identify additional PILRα ligands and further define the molecular basis for PILRα/ligand interactions. Here, we identify two novel PILRα binding partners, neuronal differentiation and proliferation factor-1 (NPDC1), and collectin-12 (COLEC12). We find that sialylated *O*-glycans on these novel PILRα ligands, and on known PILRα ligands, are compulsory for PILRα binding. Sialylation-dependent ligand recognition is also a property of SIGLEC1, a member of the sialic acid-binding Ig-like lectins. SIGLEC1 Ig domain shares ~22% sequence identity with PILRα, an identity that includes a conserved arginine localized to position 97 in mouse and human SIGLEC1, position 133 in mouse PILRα and position 126 in human PILRα. We observe that PILRα/ligand interactions require conserved PILRα Arg-133 (mouse) and Arg-126 (human), in correspondence with a previously reported requirement for SIGLEC1 Arg-197 in SIGLEC1/ligand interactions. Homology modeling identifies striking similarities between PILRα and SIGLEC1 ligand binding pockets as well as at least one set of distinctive interactions in the galactoxyl-binding site. Binding studies suggest that PILRα recognizes a complex ligand domain involving both sialic acid and protein motif(s). Thus, PILRα is evolved to engage multiple ligands with common molecular determinants to modulate myeloid cell functions in anatomical settings where PILRα ligands are expressed.

Paired receptors are cell surface proteins bearing highly similar extracellular ligand-binding domains but divergent intracellular signaling domains. Paired receptors are classified into two families, the Ig superfamily or C-type lectins, and carry out diverse functions, including fine-tuning of cellular responses, apoptosis, migration, and pathogen clearance (1–3). Human paired immunoglobulin-like receptors (PILR)[2] α and β are related type I transmembrane receptors. PILRα and -β share high similarity in their extracellular domain but contain highly divergent intracellular signaling domains and resulting functions (4, 5). PILRα is predominantly expressed in cells of the myelomonocytic lineage, including monocytes/macrophages, granulocytes, and dendritic cells (4, 6). PILRα has two cytoplasmic immunoreceptor tyrosine-based inhibitory motifs that recruit SHP-1 and SHP-2 to trigger an inhibitory signaling cascade such as reduced intracellular calcium mobilization (4, 5). PILRβ, however, associates with the immunoreceptor tyrosine-based activation motif-bearing DAP12 adaptor molecule to deliver activating signals (6). Recent evidence suggests that modulation of the PILR pathway, by triggering PILRα with an agonist antibody or by deleting PILRβ, attenuates pulmonary inflammation, emphasizing the importance of this pathway in the innate immune response (7).

PILRα ligands identified to date include mouse CD99 (mCD99) (6), PILR-associating neural protein (PANP) (8), and HSV-1 glycoprotein B (HSV-1 gB) (9). CD99 is a single chain glycoprotein that participates in the migration of leukocytes through endothelial junctions by homophilic interaction (10, 11). In mice, CD99 binds to PILRα and -β with 2.2 and 85 μM affinities, respectively (12). Two sialylated *O*-linked glycans present on mCD99 (Thr-45 and Thr-50) are crucial for inter-

[S] This article contains supplemental Figs. S1–S8.

[1] To whom correspondence should be addressed: Genentech, 1 DNA Way, South San Francisco, CA 94080. Tel.: 650-225-3402; Fax: 650-742-1521; E-mail: zarrin.ali@gene.com.

[2] The abbreviations used are: PILRα, paired immunoglobulin-like receptor α; PANP, PILR-associating neural protein; HSV-1 gB, HSV-1 glycoprotein B; ECD, extracellular domain; SPR, surface plasmon resonance; h, human; m, mouse; aa, amino acid; PBMC, peripheral blood mononuclear cell.

actions with PILR proteins (13). Sialic acid-containing glycans are abundantly expressed on cell surfaces, secreted glycoproteins, and in the extracellular matrix, where they are usually found at the exposed, nonreducing termini of oligosaccharide chains and are therefore well suited to function as ligands in cellular recognition events (14). The physiological consequence of the PILRα/CD99 interaction is not understood.

PILRα also binds to HSV-1 gB to mediate viral fusion with entry into cells (9, 15). Interestingly, expression of PILRα on cells enhances HSV-1 entry, whereas expression of PILRβ does not (16). This suggests HSV-1 gB is not a PILRβ ligand, and subtle amino acid differences between α and β play a role in ligand selectivity. Reminiscent of mCD99/PILRα interactions, PILRα recognition of gB also requires two sialylated *O*-glycans on gB (17). PILRα associates with HSV-1 gB but not with other HSV-1 glycoproteins, despite the presence of *O*-glycosylation sites on these envelope proteins (18). PILRα and PILRβ proteins do not strongly bind carbohydrate molecules in glycan microarrays (12). Therefore, PILRα does not appear to associate with glycans alone and instead seems to recognize both protein and *O*-glycan components.

Understanding common interaction themes among inhibitory receptors might provide insight into their function. Among inhibitory receptors, PILR is considered a unique family, since it bears no significant homology to other Ig superfamily members (4). Notably, a few key residues of the SIGLEC1 ligand recognition domain are found in PILRα (12). SIGLECs recognize sialylated glycans found on natural cellular ligands and also on certain pathogens that are able to synthesize or capture sialic acid from their hosts (19). The crystal structure of SIGLEC1 complexed to 3′-sialyllactose shows residues on the β-strands making multiple contacts with sialic acid, whereas relatively few contacts are formed with the adjacent carbohydrates. A highly conserved and essential arginine residue (Arg-197 in SIGLEC1) and two well conserved aromatic groups (both tryptophans) are involved in sialic acid recognition (20, 21). Likewise, the PILRα extracellular domain (ECD) shares two evolutionarily conserved arginines with SIGLECs, one of which is located in a β-strand potentially involved in ligand interactions. In this context, it is important to note that the Ig-like domain of PILRα has only 30% homology to other Ig superfamily domains, so it is possible that unique interacting domains might have evolved within PILRα (4, 5, 7, 22). Although seemingly distinct gene families, the conservation of certain residues between PILRα and SIGLECs begs the question whether these residues are involved in PILRα/ligand recognition.

We sought to elucidate how PILRα recognizes its ligands and to specifically test the requirement of the arginine shared by PILRα and SIGLEC1. Our mutational, biochemical, and homology modeling analyses show that the interaction of PILRα with its established ligands (CD99 and HSV-1 gB) requires the recognition of a conserved arginine within the ECD of PILRα combined with specific sialylated *O*-glycans on the ligands. Given this molecular mechanism of interaction, we propose that PILRα will have multiple ligands. In support of this, we observed significant binding of PILRα fusion protein to diverse primary hematopoietic cells. In addition, we report the identification of two novel binding partners of PILRα, neural proliferation differentiation and control-1 (NPDC1) and collectin-12 (COLEC12), suggesting a complex network of ligands might modulate cellular functions via PILRα.

EXPERIMENTAL PROCEDURES

Cells, Transfections, and Fusion Proteins—GenBank™ accession numbers are shown in parentheses. The DNAs encoding human PILRα (NM_013439), CD99 (NM_002414), NPDC1 (NM_015392), COLEC12 (NM_130386), mouse PILRα (NM_153510), and CD99 (NM_025584) were amplified from human and mouse splenic cDNAs. HSV-1 gB was amplified from cDNA isolated from HSV-1-infected 293T cells. Mutations were generated with a Stratagene QuikChange XL site-directed mutagenesis kit. The resulting DNA fragments were restriction digested and ligated into pRKneo with or without N-terminal FLAG or C-terminal His tags for full-length expression. 293T cells were transfected with expression constructs with Lipofectamine2000 (Invitrogen) according to the manufacturer's instructions. Two days after transfection, cells were collected for staining.

The ECDs of hCD99 (aa 1–123), mCD99 (aa 1–137), and hNPDC1 (aa 1–190) were cloned into the expression vector pRK5 as fusions to the Fc portion of murine IgG2a. The mIgG2a Fc fusion proteins were produced by transient transfection of CHO cells purified as described (23). The extracellular domains of mPILRα/mPILRαR133A (aa 1–197) and hPILRα/hPILRαR126A (aa 1–196) were produced as mIgG2a Fc fusion proteins containing two mutations known to abolish FcR binding (termed "Fc DANA") (24). Human Siglec (NM_014385) ECD (aa 1–350) fused to human IgG1 Fc was transiently expressed using the PRK vector in 293 cells and purified over Mab Select Sure (GE Healthcare). The mature N terminus (Q19) was verified using mass spectrometry.

Human NPDC1 (aa 1–190) was cloned into the expression vector pRK5 as a fusion to a C-terminal His_8 tag, and hCOLEC12 (aa 57–742) was cloned into the expression vector pRK5 with an N-terminal His_8 tag. His-tagged fusion proteins were purified with nickel nitrilotriacetic acid-agarose resin (Qiagen, 7.5 ml resin/liter) and eluted with 250 mM imidazole, 0.3 M NaCl, pH 8.0. The eluted proteins were concentrated and loaded over a Superdex 200 (GE Healthcare) gel filtration column. Appropriate fractions were pooled, concentrated, and dialyzed into PBS.

Generation of Monoclonal Antibodies—Four to 6 week old Armenian hamsters (Cytogen) or mice were immunized with 2 mg/injection each of murine and human recombinant PILRα proteins. The immunogens were resuspended in monophosphoryl lipid A/trehalose dicorynomycolate adjuvant and injected via footpad or i.p. at 3– 4-day intervals for a total of 10 boosts. Three days after the final boost, lymphocytes from immunized spleens and lymph nodes were harvested for fusion with SP2/0 myeloma cells (American Type Culture Collection) using the Cyto Pulse CEEF-50 apparatus (Cyto Pulse Sciences). Briefly, after washing twice with Cytofusion Medium C (Cyto Pulse Sciences), the isolated lymphocytes and SP2/0 cells were mixed at a 1:1 ratio and resuspended at 10 million cells/ml in Cytofusion Medium C. Electrofusion was performed according to the manufacturer's guidance. Fused cells were cultured in

ClonaCell-HY Medium C (StemCell Technologies) overnight at 37 °C in a 7% CO_2 incubator. The next day, fused cells were centrifuged and resuspended in 10 ml of ClonaCell-HY Medium C and then gently mixed with 90 ml of methylcellulose-based ClonaCell-HY Medium D (StemCell Technologies) containing HAT components. The fused cells were plated into 100-mm Petri dishes (BD Biosciences) and allowed to grow at 37 °C in a 7% CO_2 incubator. After 7–10 days, single hybridoma clones were picked by ClonePix (Genetix, United Kingdom) and transferred to 96-well cell culture plates (BD Biosciences) with 200 μl/well ClonaCell-HY Medium E (StemCell Technologies). Hybridoma culture media was changed prior to ELISA screening. All ELISA-positive clones were further screened by flow cytometry. After at least two rounds of single cell subcloning by limiting dilution, final clones were scaled up, and supernatants were collected for antibody purification. The hybridoma supernatants were purified by protein A affinity chromatography, then sterile-filtered (0.2 μm pore size, Nalgene Nunc International, New York), and stored at 4 °C in PBS. The purified mAbs were confirmed by ELISA and flow cytometry before testing in functional assays. The isotypes of purified mAbs were determined by a mouse monoclonal antibody isotyping kit (Roche Diagnostics). The isotypes of purified hamster mAbs were determined by ELISA.

Ligand Screen—The extracellular domains of hPILRα (aa 1–196) and mPILRα (aa 1–197) were cloned into the expression vector pRK5 as C-terminal fusions to alkaline phosphatase. 293T cells were transfected with PILRα-AP-pRK5 constructs using the FuGENE 6 transfection reagent (Roche Diagnostics) according to the manufacturer's instructions. Three days after transfection, supernatants were collected for screening. COS7 cells were plated in a 24-well format and transfected with 100 clones per well (Origene, human DNA library containing 20,000 genes). Two days later, cells were incubated with human or mouse PILRα-AP supernatants for 45 min at room temperature (RT). Cells were fixed with 4% paraformaldehyde for 15 min at RT and then blocked with 100 mM glycine in HBS (20 mM Hepes, pH 7.2, 150 mM NaCl) for 15 min at RT. Cells were then rinsed and incubated in HBS for 90 min at 65 °C. HBS was removed; Western Blue Substrate (Promega) was added, and color was developed for 30 min to 1 h.

MALDI-TOF MS of Permethylated O-Glycans—To release *O*-glycans by reductive β-elimination, 50 μg of concentrated protein was dissolved in 100 μl of 50 mM sodium hydroxide, 1 M sodium borohydride and incubated for ~18 h at 45 °C. Samples were acidified with glacial acetic acid and desalted using a Dowex 50X8 cation-exchange resin spin column (25). *O*-Glycans were collected in the flow-through. Residual boric acid was removed as a methyl ester by repeated evaporation (three times) with methanol in a vacuum centrifugal evaporator (Labconco). Dried glycans were subjected to two rounds of sodium hydroxide suspension/DMSO permethylation (26). Permethylated glycans were cleaned via solid phase extraction on a vacuum-driven Hypersep C18 10-mg cartridge (Thermo Scientific), followed by repeated washes with water and 5% aqueous solution of acetonitrile, and elution with a 75% aqueous solution of acetonitrile. For MALDI-TOF MS analysis, 1 μl of permethylated glycans was spotted on the stainless steel target, followed by 1 μl of "super 2,5-dihydroxybenzoic acid" matrix, and samples were briefly dried using vacuum (25). Spectra were acquired in a positive mode on a Bruker UltraFlex MALDI-TOF/TOF instrument and calibrated with permethylated glucose homopolymer mixture (ProZyme). Mass-based glycan composition assignment was performed using GlycoMod (27).

Radioligand Cell Binding Assay—The affinity of hPILRα-Fc for hNPCD1 expressed on 293T cells was determined in a competitive equilibrium radioligand cell binding assay. Human PILRα-Fc was iodinated with ^{125}I using the Indogen method, and free ^{125}I-Na was removed using a NAP-5 column. 50-μl competition reaction mixtures containing a fixed concentration of iodinated ligand and decreasing concentrations of serially diluted, unlabeled ligand were placed into 96-well plates in triplicate. To each well, 293T cells transiently expressing hNPCD1 were added at a density of 200,000 cells/0.2 ml of binding buffer (Dulbecco's modified Eagle's medium with 1% bovine serum albumin, 230 nM IgG2a, 50 mM Hepes, pH 7.2, and 2 mM sodium azide). The final concentration of the iodinated protein in each competition reaction was 700 pM (340,000 cpms per 0.25 ml). The final concentration of the unlabeled ligand in the competition reaction varied, starting at 1000 nM and decreasing by 1–2-fold dilution for 10 concentrations, and included a zero added buffer only sample. Competition reactions were incubated for 2 h at room temperature, then transferred to a Millipore Multiscreen filter plate (Billerica, MA), and washed four times with binding buffer to separate free from bound iodinated antibody. The filters were counted on a Wallac Wizard 1470 γ-counter (PerkinElmer Life Sciences). The binding data were evaluated using NewLigand software (Genentech), which uses the fitting algorithm of Munson and Robard to determine the binding affinity of the antibody (28). The calculated equilibrium K_D value for the replicates assays was 41 and 57 nM.

Equilibrium Affinity Measurement by Surface Plasmon Resonance (SPR)—Equilibrium binding analysis was conducted using ProteonXPR36 (Bio-Rad). Human COLEC12-His was immobilized on six parallel flow cells on a Proteon GLC sensor chip at 6400 response units by 1-ethyl-3-(3-dimethylaminopropyl)carbodiimide hydrochloride/*N*-hydroxysuccinimide amine coupling, and the chip surface was deactivated by ethanolamine after immobilization. 1-ethyl-3-(3-dimethylaminopropyl)carbodiimide hydrochloride/*N*-hydroxysuccinimide treatment without protein was used to generate the reference flow cells. Human PILRα-Fc protein was diluted to the appropriate concentrations in PBST (PBS + 0.005% Tween 20) and injected at 80 μl/min at room temperature along with a PBST only control over the immobilized proteins for 5 min. Reference subtracted data were analyzed using the Bio-Rad Proteon equilibrium binding software. The equilibrium-binding model was applied using global R_{max} and K_D fitting. The equilibrium K_D was calculated at 1.1 μM (R_{max} = 357, χ^2 = 25 response units).

Desialylation Procedure—The analytes used for Biacore binding studies were treated with sialidase A (Prozyme) to cleave sialic acids from the proteins. For 100 μg of glycoprotein, 14 μl of deionized water, 4 μl of 5× reaction buffer, 2 μl of sialidase A were added and incubated for 1 h at 37 °C. The

treated protein was diluted 1:5 into 20 mM Tris, pH 8, 1 mM Azide and run over a Mono Q column (GE Healthcare) to separate the enzyme from the protein. The appropriate fractions from the Mono Q run were pooled and used for the Biacore binding studies. To remove sialic acid from cell surfaces, cells were incubated with sialidase A in PBS, pH 6, at 37 °C, for 3 h. PILRα-Fc binding to sialidase A-treated cells was detected by flow cytometry.

Sialidase-Treated Binding Analysis—The binding of selected proteins was determined by SPR using a Biacore 3000 biosensor system (GE Healthcare). Human PILRα (25 μg/ml in 10 mM sodium acetate, pH 4.5) was immobilized to a CM5 sensor chip (GE Healthcare) by amine coupling chemistry at a flow rate of 5 μl/min. The control flow cell was prepared using buffer without the ligand. The affinity measurements were carried out in HBS-EP running buffer (10 mM Hepes, pH 7.4, 150 mM NaCl, 3 mM EDTA, 0.005% P20 surfactant) at a flow rate of 20 μl/min with a 3-min injection time. Sensor surfaces were regenerated with 10 mM glycine, pH 3, for 2 min between runs. The test proteins were diluted in HSB-EP buffer to 1 μM concentrations. Data were analyzed with BIAevaluation 4.1 software with subtraction of the control cell binding from sensograms.

HSV-1 Infection of 293T Cells—HSV-1 KOS strain (ATCC) was propagated in Vero cells. 293T cells were grown to 80–90% confluence and infected with HSV-1 at a multiplicity of infection of 0.1 plaque-forming units/ml. After 1 h of adsorption at 37 °C, the virus inoculums were removed and replaced with minimal essential medium supplemented with 5% FBS, 100 units/ml penicillin, and 100 mg/ml streptomycin. Twenty four hours after infection, cells were harvested and analyzed for gB expression and PILRα-Fc staining by flow cytometry.

Flow Cytometry—Cells were stained with a saturating dose of PILRα or ligand fusion proteins. Tagged fusions were detected with FITC-conjugated anti-mouse IgG2a (Pharmingen) or phycoerythrin-conjugated anti-poly-His (R & D Systems) with anti-ragweed mIgG2a (in-house) as control. For cell surface expression of transfected genes, cells were further stained with goat polyclonal antibodies against mCD99 or hCD99 (R & D Systems) followed by allophycocyanin-conjugated donkey anti-goat IgG (R & D Systems); N-FLAG tagged hNPDC1 expression was detected with biotin-conjugated anti-FLAG (Sigma) followed by APC-conjugated streptavidin (Pharmingen); C-His-tagged hCOLEC12 expression was detected with phycoerythrin-conjugated anti-poly-His (R & D Systems). Mouse PILRα expression was detected with in-house-generated hamster anti-mPILRα followed by APC-conjugated goat anti-hamster IgG (Jackson ImmunoResearch). Human PILRα expression was detected with in-house-generated mouse anti-hPILRα followed by purified goat anti-mIgG1 (Southern Biotech) and APC-conjugated donkey anti-goat IgG (R & D Systems). HSV-1-infected 293T cells were incubated with anti-gB (mAb H1817, Novus Biologicals) followed by an APC-conjugated anti-mouse IgG (Jackson ImmunoResearch). Cells were fixed with 4% paraformaldehyde before analysis. For the binding of PILRα fusion proteins to sialidase A-treated and nontreated primary cells, C57BL/6 (The Jackson Laboratory) mouse thymocytes and peripheral lymph node cells, and human PBMCs were stained with PILRα fusion proteins followed by FITC-conjugated anti-mouse IgG2a. Mouse lymph node cells were further stained with phycoerythrin-conjugated anti-CD8. PBMCs were further stained with APC-conjugated anti-CD3 (all Pharmingen). Cell acquisition was performed on a FACScalibur (BD Biosciences), and data were analyzed with Flowjo software.

Homology Modeling—The PILRα sequence was aligned with the N terminus of mouse sialo-adhesin from Protein Data Bank code 1QFO using the MOE2011.10 Protein Align application (29). Blosum62 was used as the alignment matrix, with tree-based build-up, gap start penalty of 7 and gap extend penalty of 1, iteration limit of 100, and failure limit of 10. The aligned structures were used to build a homology model using the homology model application in MOE2011.10. The three dimensional structure of the first chain in SIGLEC1 was used as the template, with the ligand atoms used as the "environment" during model building (20, 21). The C- and N-terminal outgaps were not built. A total of 25 models were built with fine minimization, and the final model was processed in Protonate3D to detect the correct protonation states and then finely minimized. The Merck force field (MMFF94×) with Born solvation method was used to reproduce the small molecule interactions of the active site. The active site/ligand interactions of SIGLEC1 and those of the PILRα model were rendered using the ligand interaction diagram application of MOE2011.10 (30). The active site/ligand contacts are coded according to Table 1.

Glycan Binding Assay—Each well of a 96-well plate (Nunc) was coated with 100 μl of 5 μg/ml protein A (Sigma) in 50 mM sodium bicarbonate buffer, pH 9.5, at 4 °C overnight. Plates were washed twice and left to block in ELISA buffer (20 mM Hepes-NaOH, pH 7.2, 125 mM NaCl, 0.02% NaN3, 1% BSA) for 1 h at RT. Subsequent steps were performed at RT, and each addition of protein was followed by three washes of ELISA buffer (150 μl/well). First, human PILRα-Fc, SIGLEC-7, or murine IgG2a or human PILRαR126A-Fc (2 μg/ml in ELISA buffer) were coated for 2 h, followed by a 2-h incubation with PAA-Bio probes (Glycotech, 0.5 μg/ml in ELISA buffer). Next, streptavidin-alkaline phosphatase (Invitrogen, 1 μg/ml in ELISA buffer) was added for 1 h. Wells were developed using 100 μl/well of *p*-nitrophenyl phosphate liquid substrate system (Sigma) for 30 min in the dark. Plates were read at 405 nm with a Tecan Safire 2 multiwell plate reader. Binding for each receptor-ligand pair was tested in triplicate. Wells containing glycan probes but no protein were used to gauge background signal.

Glycan Competition Assay—The binding of selected proteins was determined by SPR using a Biacore 3000 biosensor system (GE Healthcare). Human NPDC1 (15 μg/ml in 10 mM sodium acetate, pH 5) was immobilized to a CM5 sensor chip (GE Healthcare) by amine coupling chemistry at a flow rate of 5 μl/min. The control flow cell was prepared using the buffer without the ligand. The affinity measurements were carried out in HBS-P running buffer (10 mM Hepes, pH 7.4, 150 mM NaCl, 0.005% P20 surfactant) at a flow rate of 20 μl/min with a 3-min injection time. Sensor surfaces were regenerated with 10 mM glycine, pH 2.0, for human NPDC1. There was a 30-s injection time and a 2-min stabilization

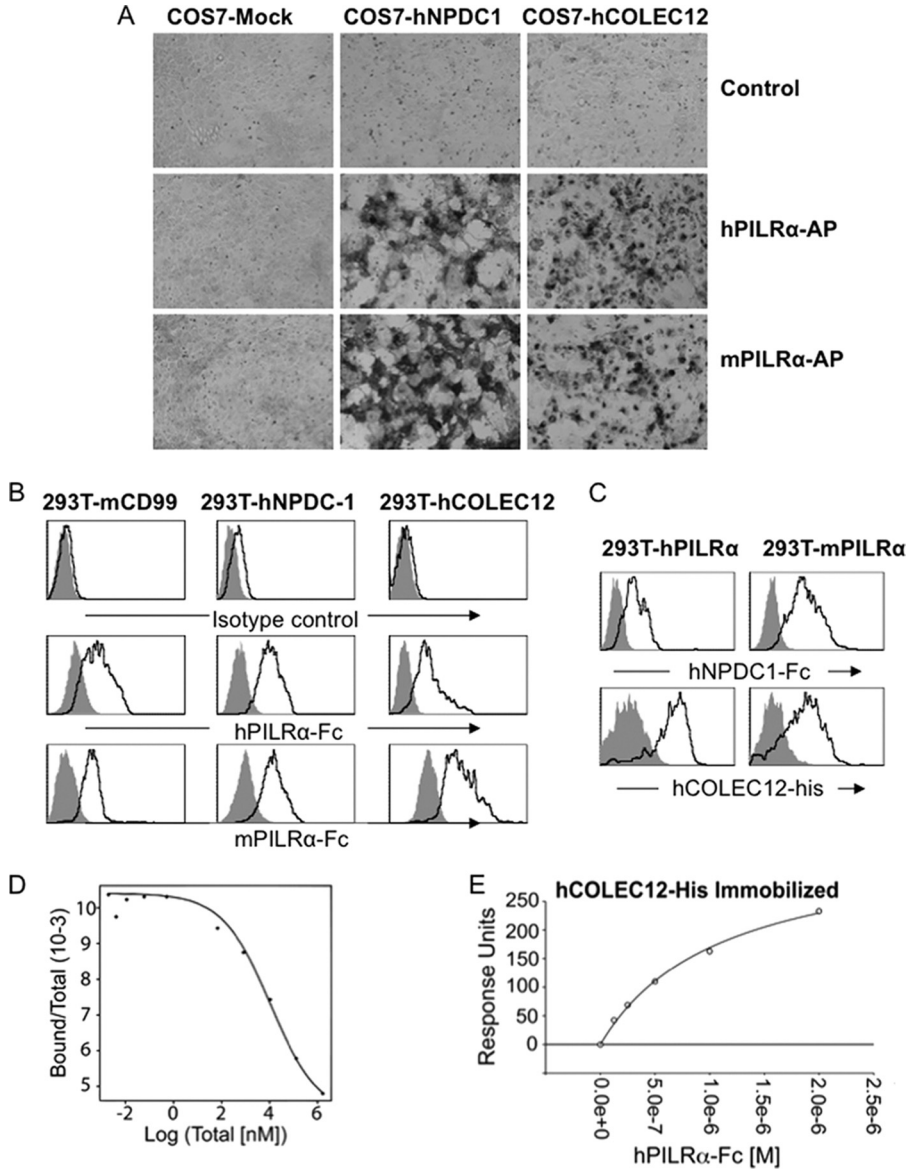

FIGURE 1. **NPDC1 and COLEC12 are novel ligands of PILRα.** *A,* COS7 cells were transfected with hNPDC1 and hCOLEC12 expression vectors and then stained with hPILRα-AP, mPILRα-AP, and control supernatants followed with alkaline phosphatase substrate. *B,* 293T cells were transfected with mCD99, hNPDC1, and hCOLEC12, and the transfectants were stained with isotype control, hPILRα-Fc, or mPILRα-Fc (*black line*). Binding to mock transfectants (*gray area*) represents background binding. Transfected ligand expressing cells were gated, and their binding to PILRα-Fc is shown. *C,* 293T cells were transfected with human and mouse PILRα, and the transfectants were stained with hNPDC1-Fc or hCOLEC12-His (*black line*). Binding to mock transfectants (*gray area*) represents background binding. PILRα-positive cells were gated, and ligand fusion staining was shown. *D,* radioligand assays were used to determine the equilibrium binding affinity of hPILRα-Fc to hNPDC1 transiently expressed on 293T cells. ^{125}I-Labeled hPILRα-Fc was allowed to bind to cells in the presence of increasing amounts of unlabeled hPRILα-Fc. The average equilibrium K_D value from two replicate assays was 49 nM. *E,* SPR equilibrium binding analysis of hPILRα-Fc binding to immobilized hCOLEC12 is shown. The equilibrium K_D value for hPILRα/hCOLEC12 was 1.1 μM.

time between runs. The test proteins were diluted in HSB-P buffer to the appropriate concentrations. Data were analyzed with BIA evaluation 4.1 software with subtraction of the control cell binding from sensograms.

RESULTS

NPDC1 and COLEC12 Are Novel Ligands of hPILRα—It has been shown that PILRα has multiple ligands, including mCD99, HSV-1-gB, and the recently identified PANP, and the presence of sialylated *O*-glycans on these molecules is required for their binding to PILRα (8, 12, 13, 17). Given the mechanism by which PILRα recognizes its ligands, we speculated that PILRα would interact with additional novel ligands. We screened a human cDNA expression library with an alkaline phosphatase-tagged hPILRα. In doing so, we found that hPILRα-AP bound to NPDC1- and COLEC12-expressing cells (Fig. 1*A*). Both mouse and human PILRα-AP were able to bind each other, suggesting a conserved interaction domain mediates PILRα binding to these proteins. NPDC1 is a type I transmembrane protein and has been identified as a neuron-specific gene involved in the control of cell proliferation and differentiation (31). COLEC12 is a type II transmembrane collectin family member also known as collectin placenta 1 (CL-P1) (32) and scavenger receptor with C-type lectin type I (33).

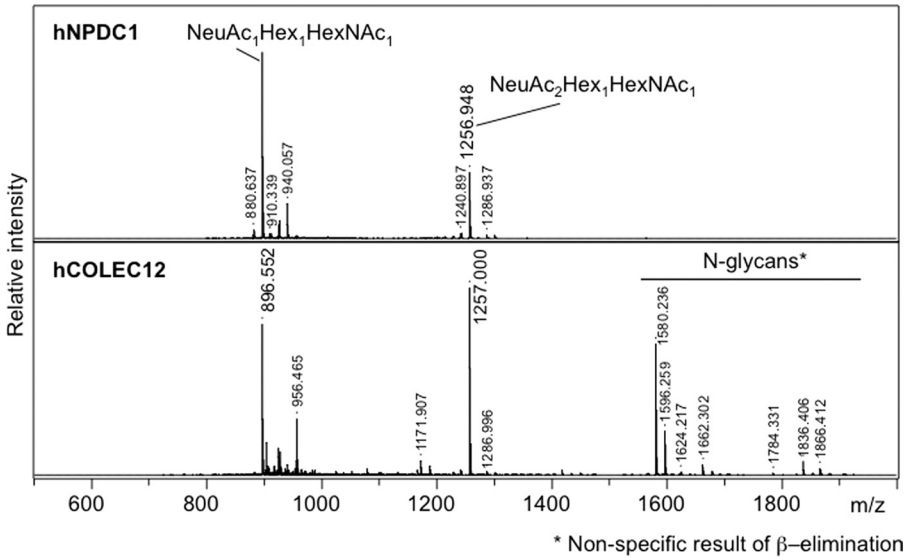

FIGURE 2. **Human NPDC1 and COLEC12 are glycosylated with sialylated glycans.** Comparison of MALDI-TOF MS spectra of permethylated *O*-glycans, released by reductive β-elimination, from human NPDC1-Fc and human COLEC12-His is shown. Molecular ions of permethylated glycans (glycan alditols) were detected in positive ion mode as sodium adducts $(M + Na)^+$.

To confirm the binding of PILRα to cell surface hNPDC1 and hCOLEC12, we expressed N-terminal FLAG-tagged hNPDC1 or C-terminal His-tagged hCOLEC12 in 293T cells, and then we tested mPILRα-Fc and hPILRα-Fc binding by flow cytometry. mCD99-transfected cells were used as a positive control. Both mPILRα-Fc and hPILRα-Fc bound to mCD99-, hNPDC1-, and hCOLEC12-expressing cells (Fig. 1*B*). Similar results were obtained in the converse experiment, in which hNPDC1-Fc and hCOLEC12-His recombinant proteins were applied to PILRα-transfected cells. Again, both hNPDC1-Fc and hCOLEC12-His bound to human and mouse PILRα (Fig. 1*C*). Using an equilibrium competition radioligand assay, the affinity (K_D) of hPILRα-Fc binding to the cell surface-expressed hNPDC1 was determined to be 49 nM (Fig. 1*D*). We were unable to determine the affinity of COLEC12 for PILRα using this method, presumably due to a low affinity interaction. We repeated these measurements using SPR (Fig. 1*E*). Through this method, the equilibrium K_D of the PILRα:COLEC12 was determined to be 1.1 μM. Taken together these studies demonstrate the binding of PILRα to human NPDC1 and COLEC12 is specific and conserved across species.

O-Glycosylation of Human NPDC1 and COLEC12 Is Required for Their Binding to PILRα—The presence of sialylated *O*-glycans is required for PILRα to bind its known ligands, including mCD99, HSV-1 gB, and PANP (8, 13, 17). Human NPDC1 and COLEC12 have multiple potential *O*-glycosylation sites when analyzed using the NetOGlyc 3.1 prediction server (34). hNPDC1 does not have any potential *N*-glycosylation sites, although hCOLEC12 has multiple sites. To determine whether both proteins are indeed *O*-glycosylated, they were analyzed by MALDI-TOF MS. MALDI-TOF MS analysis of permethylated *O*-glycans released by reductive β-elimination from hNPDC1-Fc and hCOLEC12-His confirmed the presence of *O*-glycans. Both hNPDC1 and hCOLEC12 showed qualitatively similar *O*-glycosylation profiles and two major mono- and di-sialylated *O*-glycans, having the composition $NeuAc_1Hex_1HexNAc_1$ and $NeuAc_2Hex_1HexNAc_1$ (Fig. 2). In addition, analysis of hCOLEC12 by a combination of HPLC charge profiling of fluorescent 2-aminobenzoic acid-labeled glycans and MALDI-TOF of permethylated unlabeled glycans (supplemental Fig. S1) also demonstrated its complex *N*-glycosylation profile. Neutral glycans were mostly of the high mannose type (predominantly Man-5) and complex a fucosylated or core-fucosylated bi-, tri-, and tetra-antennary glycan, galactosylated to various degrees. Negatively charged glycans were a mixture of core-fucosylated bi-, tri-, and tetra-antennary *N*-glycans, mostly fully galactosylated sialylated to different extent (from 1 to 4 sialic acid residues).

To test whether sialylated glycans on NPDC1 and COLEC12 are required for their binding to PILRα, we performed SPR analysis using Biacore with hNPDC1 and hCOLEC12 fusion proteins with and without sialidase A treatment. Before sialidase A treatment, the proteins showed good binding responses to hPILRα (Fig. 3). However, after sialidase A treatment, the proteins showed little or no binding to hPILRα (Fig. 3). mCD99 was used as a control and showed similar results to both hNPDC1 and hCOLEC12 (Fig. 3). These studies suggest that the sialylated glycans on hNPDC1 and hCOLEC12 are required for their binding to hPILRα.

Transfer of Mouse CD99 PKAPT Motif to Human CD99 Restores PILRα Binding—Mouse PILRα binds to mCD99 with relatively low affinity (6, 12). However, it is unclear whether PILRα can bind human CD99. To test this, we expressed mouse or human CD99 in 293T cells and stained with PILRα-mIgG2a (PILRα-Fc) fusion proteins. We found that both mouse and human PILRα-Fc fusions bound to mCD99 transfectants, but neither protein bound to hCD99 transfectants (Fig. 4*A*). This suggests that the CD99 interaction with PILRα is not conserved, at least between humans and mice. However, as described below, we hypothesized that a conserved PILRα interaction domain between mouse and human PILRα may mediate its binding to mCD99.

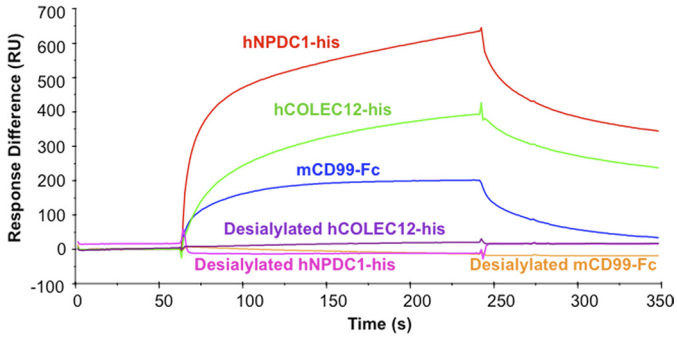

FIGURE 3. **Sialylated glycans on NPDC1 or COLEC12 are required for their binding to PILRα.** The binding of selected proteins to hPILRα was determined by SPR. Human PILRα-Fc (25 μg/ml) was immobilized to a CM5 sensor chip resulting in 11,551 resonance units (*RU*) bound to chip. Fusion proteins with and without sialidase A treatment were used as analytes (1 μM). Sensograms were corrected for response difference between active and reference flow cell.

The differential binding of mouse and human CD99 to PILRα may be the result of the low sequence identity between CD99 homologs (about 41% in the extracellular domain, supplemental Fig. S2) and/or the differences in glycosylation (type and/or number of glycans). It has been shown that sialylated *O*-linked glycans on mCD99 play an essential role in PILRα binding (13). hCD99 has been reported to be *O*-glycosylated (35), and like mCD99, it does not bear any potential *N*-glycosylation sites. We investigated the possibility that lack of PILRα binding to hCD99 is due to it carrying a distinct *O*-glycosylation pattern. We first compared profiles of *O*-glycans from human and mouse CD99-Fc fusion proteins. *O*-Glycans were released by reductive β-elimination and permethylated prior to analysis by MALDI-TOF MS. Comparison of MALDI-TOF spectra (Fig. 4*B*) demonstrated qualitatively similar *O*-glycosylation profiles of human and mouse CD99, and they are similar to those determined for hNPDC1 and hCOLEC12. The composition of the observed *O*-glycans is consistent with the presence of sialylated Galβ1–3GalNAc core 1 structures, typical of CHO cell-expressed glycoproteins (36, 37).

Because *O*-glycans of human and mouse CD99 did not differ qualitatively, we next examined whether there might be a difference in the number of *O*-glycans present on each of the proteins. LC-MS analysis of reduced fusion proteins (with and without PNGase F and sialidase digestion) showed that hCD99-Fc carried two *O*-glycans and mCD99-Fc carried three *O*-glycans with the composition $NeuAc_{1-2}Hex_1HexNAc_1$. In the case of mCD99, two adjacent *O*-glycosylation sites, Thr-45 and Thr-50 (NMKP$\underline{T}^{45}$PKAP$\underline{T}^{50}$PKKPS) are relevant for PILRα recognition (13). Sequence alignment of human and mouse CD99 showed that Thr-41 of hCD99 corresponds to the Thr-45 *O*-glycosylation site of mCD99 and that hCD99 lacks the second potential *O*-glycosylation site corresponding to Thr-50 of mCD99 (supplemental Fig. S2). Therefore, we performed LC-MS tryptic peptide mapping of hCD99-Fc to determine the localization of *O*-glycans and to examine whether the peptide containing Thr-41 is indeed *O*-glycosylated. Two sialylated glycopeptides with following sequence were detected, APDGGFLDLSDALPDNENKKPTAIPK (hCD99-derived) and GPTIKPCPPCK (mIgG2a Fc-derived) (supplemental Fig. S3). Each glycopeptide was glycosylated with a single $NeuAc_{1-2}Hex_1HexNAc_1$ *O*-glycan. The presence of two sialylated glycopeptides was consistent with the LC-MS analysis of reduced hCD99-Fc. The detected sialoglycopeptide APDGGFLDL$\underline{S}$DALPDNENKKP$\underline{T}^{41}$AIPK contained Thr-41 and a Ser residue that potentially could be *O*-glycosylated. However, the exact site of *O*-glycosylation could not have been sequenced through the performed type of LC-MS experiment. The presence of an *O*-glycan on the GPTIKPCPPCK peptide is consistent with the previous report of it being *O*-glycosylated in the truncated version of mouse IgG2a (38).

Our results indicated that human and mouse CD99 have similar sialylated core 1 *O*-glycans ($NeuAc_{1-2}Hex_1HexNAc_1$) but that the presence of such glycans *per se* on hCD99 is not sufficient for PILRα binding. In addition, it is possible that certain protein interacting domains or conformations have diverged between mouse and human CD99 (supplemental Fig. S2). One major difference between the mouse and human CD99 glycosylation is that mCD99 has two *O*-glycosylation sites (Thr-45 and Thr-50) (13) *versus* one in the human counterpart (Thr-41). It is possible that certain motifs or conformations have diverged between mouse and human CD99 (supplemental Fig. S2). We asked whether the introduction of the mCD99 region ^{46}PKAPT^{50} (PKAPT) into hCD99 could confer binding of PILRα. We expressed full-length mCD99, hCD99, and hCD99PKAPT in 293T cells, and we again tested the binding of hPILRα-Fc or mPILRα-Fc by flow cytometry. We found that insertion of the mCD99 PKAPT motif into hCD99, directly following the Thr-41 *O*-glycosylation site, conferred binding activity of human or mouse PILRα to hCD99PKAPT-expressing cells (Fig. 4*C*). Surprisingly, this interaction was similar in magnitude to human or mouse PILRα binding to mCD99. This suggests that PKAPT peptide is sufficient to render hCD99 to bind PILRα likely by providing additional *O*-glycosylation sites and/or certain protein determinants.

Conserved Arginine Residue in PILRα Is Required for Binding to Its Ligands—Sialylated glycan modifications appear to be a general feature of all known PILRα ligands and coincidently a few other ligands of receptors such as SIGLECs (8, 12, 13, 17, 19). A conserved arginine in the ECD of SIGLECs plays a critical role in their binding to sialic acid (20, 39, 40). The PILRα ECD has two similar arginines (human Arg-96 and Arg-126 and mouse Arg-103 and Arg-133) that are highly conserved across species (Fig. 5*A*). The second residue (mouse Arg-133 and human Arg-126) corresponds to the critical arginine in SIGLECs that is required for their binding sialic acid on ligands (20). The Arg-126 of hPILRα and the Arg-133 of mPILRα are not Ig-fold stabilizing residues (Fig. 5*A*) (4). We examined whether mutation of Arg-133 and Arg-126 to alanine in mouse or human PILRα affects their ligand binding activity. First, we tested the binding of ligand fusion proteins mCD99-Fc, hNPDC1-Fc, and hCOLEC12-His to cell surface-expressed wild type (WT) or mutated hPILRαR126A and mPILRαR133A. The mutation did not affect cell surface expression of either human or mouse PILRα (supplemental Fig. S4). We found that all fusion proteins bound to cells transfected with the wild type (WT) versions, but not to cells transfected with either hPILRαR126A or mPILRαR133A (Fig. 5*B*), suggesting Arg-126 in hPILRα and Arg-133 in mouse PILRα are required for

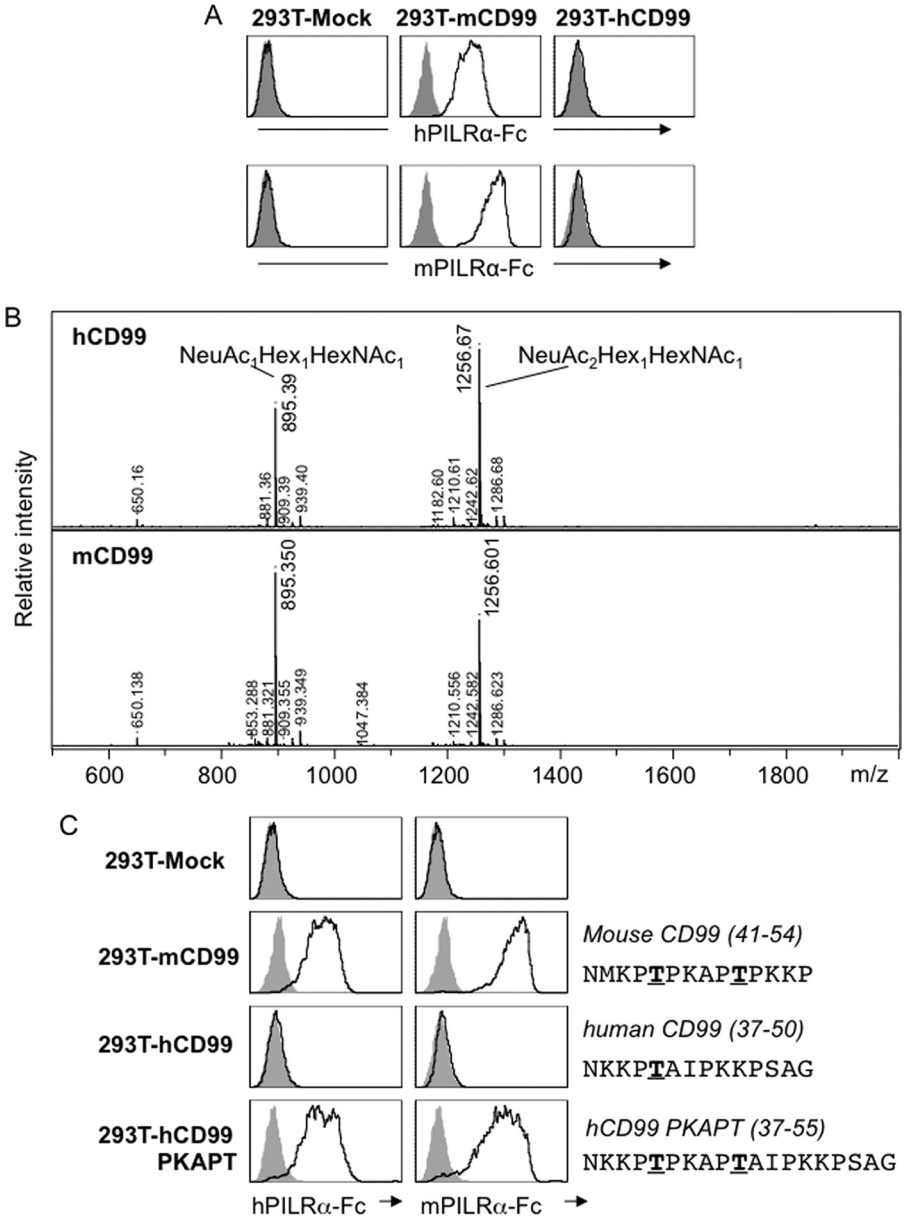

FIGURE 4. **PILRα binds to mouse but not human CD99 and transfer of the mouse CD99 PKAPT motif to human CD99 restores PILRα binding.** *A,* 293T cells were transfected with mouse and human CD99 expression vectors, and the transfectants were stained with hPILRα-Fc (*black line*), mouse PILRα-Fc (*black line*), or control Ig (*gray area*). CD99-expressing cells were gated, and their binding to PILRα-Fc is shown. *B,* comparison of profiles of *O*-glycans from human and mouse CD99-Fc fusion proteins. *O*-Glycans were released by reductive β-elimination, permethylated, and then analyzed by MALDI-TOF MS. *C,* 293T cells were transfected with either mouse or human CD99 or human CD99 with the mouse PKAPT motif inserted after Thr-41. The transfectants were stained with hPILRα-Fc (*black line*), mouse PILRα-Fc (*black line*), or control Ig (*gray area*). The amino acid sequences of regions surrounding the *O*-glycosylated threonines (*underlined* and *bold*) in mouse and human CD99 are shown.

PILRα/ligand interactions. We also generated WT and arginine mutant human and mouse PILRα-Fc fusion proteins and examined their binding to cell surface expressed ligands. WT human and mouse PILRα-Fc bound to mCD99-, hNPDC1-, hCOLEC12-, and HSV-1 gB-transfected cells, whereas hPILRαR126A-Fc and mPILRαR133A-Fc did not (Fig. 5*C*). Because gB expression can be detected on HSV-1-infected cells 24 h after infection (Fig. 5*D, left panel*), we additionally tested whether each version of human or mouse PILRα-Fc bound to HSV-1-infected cells. Again, we observed the binding of only the WT, but not the mutant, version to HSV-1-infected 293T cells (Fig. 5*D, right panels*). These studies further support an important role for this conserved arginine residue in PILRα/ligand interactions.

To better quantify the difference in binding affinities between WT and mutant PILRα variants to ligands, we performed SPR analysis. The WT hPILRα-Fc and hPILRαR126A-Fc were immobilized on a chip, and their binding to hNPDC1, hCOLEC12, and mCD99 was compared (Fig. 5*E*). All three proteins showed strong binding to WT hPILRα (Fig. 5*E*). However, little or no binding was observed with mutant hPILRα, suggesting the conserved arginine is necessary for the interaction (Fig. 5*E*).

Our data suggest that PILRα/ligand interactions require a conserved arginine on PILRα and specific sialylated decora-

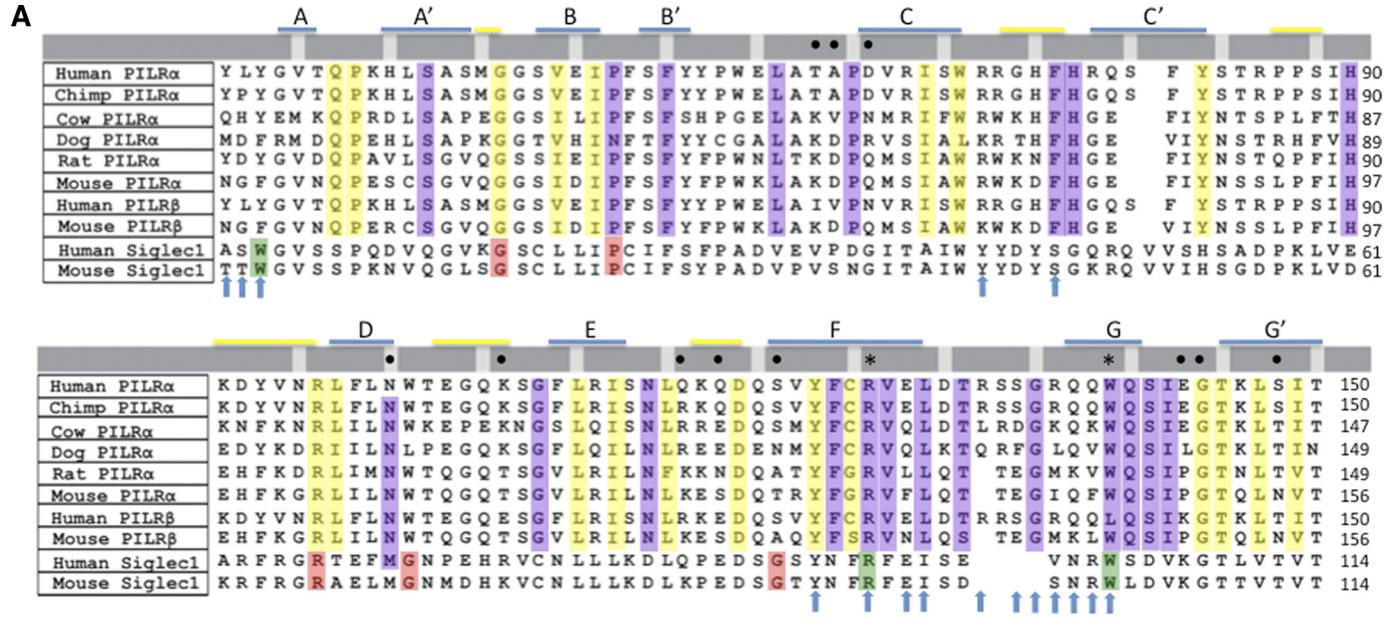

FIGURE 5. **A conserved arginine in PILRα is required for ligand binding.** *A,* amino acid sequence alignment of PILRα from various species, PILRβ and the N terminus of SIGLEC1. The positions of Ig fold residues are shown in *yellow* based on comparison with Igκ/λ and TCRβ V set Ig domains. Conserved non-Ig PILRα residues are shown in *purple*. SIGLEC1 residues involved in the sialic acid-binding are in *green*. SIGLEC residues conserved across the family are shown in *red*. *Asterisks* represent PILRα amino acids that are important for sialic acid interaction. *Blue arrows* denote the positions corresponding to active sites of the SIGLEC1 crystal structure and PILRα homology model. The *underlined* segments designate β-strands within PILRα. *Black circles* represent PILRα residues that were mutated to screen for HSV-1/gB binding by others (16). The pairwise percentage residue identity between PILRα and SIGLEC1 was 23%. *B,* 293T cells were transfected with WT human and mouse PILRα (*blue line*), or human PILRαR126A and mouse PILRαR133A (*red line*) expression constructs, and the transfectants were stained with mCD99-Fc, hNPDC1-Fc, or hCOLEC12-His. Background binding to mock transfectants is shown in *gray*. PILRα-positive cells were gated, and ligand fusion staining is shown. *C,* 293T cells were transfected with mouse CD99, human NPDC1 and COLEC12, or HSV-1 gB expression vectors, and transfectants were stained with hPILRα-Fc or mPILRα-Fc (*blue line*), hPILRαR126A-Fc, or mPILRαR133A-Fc (*red line*) or control IgG (*gray area*). Ligand-expressing cells were gated, and PILRα-Fc staining was shown. *D,* 293T cells were infected with HSV-1. *Left panel,* 24 h later, gB expression in HSV-1 (*black line*) or mock (*gray area*) infected cells is shown; *right panel,* hPILRα-Fc or mPILRα-Fc (*blue line*), hPILRαR126A-Fc, or mPILRαR133A-Fc (*red line*) binding to HSV-1 infected cells is shown, and their binding to mock transfectants (*gray area*) is shown as background binding. *E,* binding of ligand fusion proteins to wild type and arginine mutated human PILRα. The binding of selected proteins to hPILRα was determined by SPR. Human PILRα-Fc and PILRαR126A-Fc was immobilized to a CM5 sensor chip resulting in 10,540.0 response units (*RU*) bound to the chip. Fusion proteins were used as analytes (1 μM). Sensograms were corrected for response difference between active and reference flow cell. *F,* binding of hPILRα-Fc or mPILRα-Fc (*blue line*) and hPILRαR126A-Fc or mPILRαR133A-Fc (*red line*) to total human PBMC and T cells (*left panels*), mouse thymocytes, and $CD8^+$ T cells (*right panels*) is shown, and the binding of isotype control to these cells is shown in *gray*.

tions on the ligands. Because sialylation occurs naturally on many cell surface proteins, we predicted that hPILRαR126A/mPILRαR133A proteins would not recognize ligands present on the surface of primary cells. To test this, we stained mouse and human hematopoietic cells with human or mouse PILRα-Fc. We found that both human and mouse PILRα-Fc bound to the majority of human PBMCs (Fig. 5*F*, *left upper panels*) and also showed strong binding to human T cells (Fig. 5*F, left, lower panels*). For murine cells, PILRα-Fc fusions bound well to thymocytes and $CD8^+$ peripheral T cells (Fig. 5*F, right panels*). However, neither hPILRαR126A-Fc nor mPILRαR133A-Fc bound to human PBMCs (Fig. 5*F, left panels*), mouse thymocytes, or peripheral T cells (Fig. 5*F, right panels*). These results suggest the conserved arginine residue within mouse and human PILRα is required not only for binding to ligands expressed via transfection but also to ligands present on primary cells.

Role of Sialic Acid in Mediating PILRa/Ligand Interactions—To examine the contribution of sialic acid to PILRα/ligand interactions on primary cells, we treated cells with sialidase A, a broad specificity enzyme capable of cleaving a variety of sialic acid linkages. We found that sialidase A treatment of human PBMCs (Fig. 6*A, left panels*), mouse thymocytes, as well as $CD8^+$ T cells (Fig. 6*A, right panels*) abolished both hPILRα-Fc and mPILRα-Fc binding. The removal of sialic acid from cell surfaces was confirmed by loss of binding by human SIGLEC, which is known to directly bind sialic acid (supplemental Fig. S5*A*) (19). Sialidase A treatment did not significantly affect the global expression of cell surface markers, as gauged by CD3 and CD8 levels (supplemental Fig. S5*B*). We conclude that sialic acid is an essential component of PILRα ligands naturally expressed by primary cells.

We next tested whether PILRα directly binds to sialic acid in a manner similar to SIGLECs (19). Using SPR analysis, we examined whether PILRα binding to hNPDC1-His can be inhibited by 3′-siallylactose or 6′-siallylactose, two common monovalent sialylated carbohydrates containing sialic acid (Neu5Ac) in α2–3 and α2–6 linkage, respectively. 6′-Siallylactose, tested in the concentration range up to 125 mM, clearly inhibited PILRα binding to NPDC1 (Fig. 6*B*, *top panel*). Only partial inhibition of PILRα with NPDC1 was achieved even at high concentrations of 6′-siallyllactose suggesting that other motifs mediate PILRα NPDC1 interaction. However, no appreciable inhibition of binding was achieved with the highest concentration of competing lactose carbohydrate (Fig. 6*B*, *bottom right*). 3′-Siallylactose, tested in the similar concentration range as 6′-siallylactose, did not significantly inhibit PILRα binding to hNPDC1-His (Fig. 6*B*, *bottom left*). Furthermore, we used an

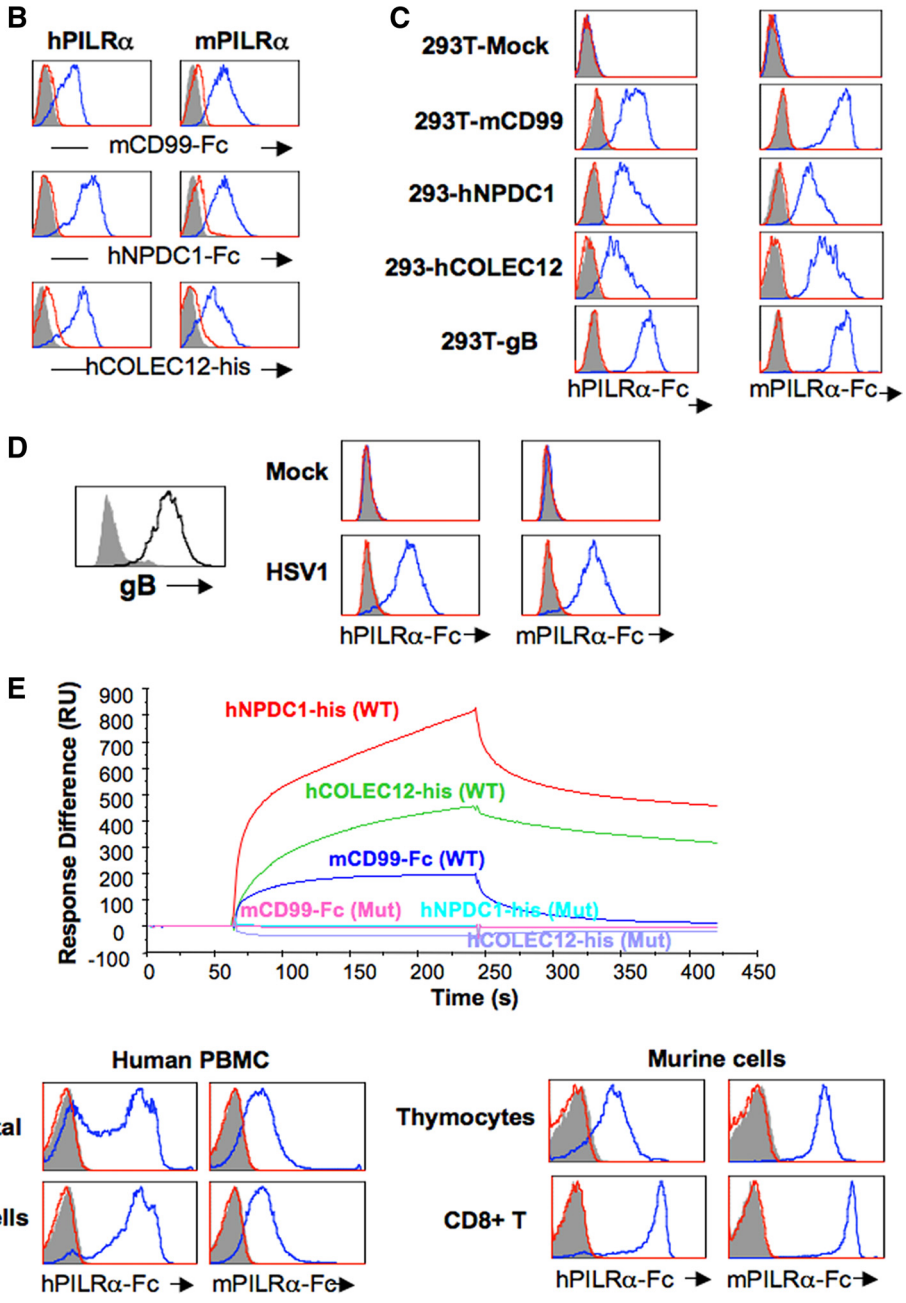

FIGURE 5—*continued*

ELISA-based assay with selected multivalent sialylated glycan probes, including glycan structure identified on the ligands, in attempt to show a direct binding of PILRα to sialylated glycans. SIGLEC was used as a positive control. Siglec-Fc strongly bound to oligomeric probes Neu5Acα2–6GalNAc-PAA-biotin and Neu5Acα2–8Neu5Acα2–8Neu5Ac-sp-PAA-biotin (Neu5Ac)3 compared with other probes (supplemental Fig. S6). However, hPILRα did not show significant binding to any of the glycan probes. These results suggested that although PILRα may have a higher specificity toward sialic acid present in α2–6 linkage, it is not a lectin. PILRα likely binds to a more complex structure involving both sialic acid and a protein determinant (see below).

Modeling PILRα/Ligand Interaction Domain—Our study identifies Arg-126 (mouse Arg-133) as a critical contact residue in hPILRα (Fig. 5). Others have shown that Trp-139 is also important in mediating hPILRα interaction with its ligand gB (16). Given the similarities of the binding residues between PILRα and the SIGLEC family, we built a homology model of PILRα to gain insights into its contact residues (Fig. 7, Table 1, and supplemental Fig. S7). The crystal structure of SIGLEC1 (PDB code 1QFO) was used as a template, whereas the ligand atoms (see supplemental Fig. S7*A*) for sialic acid ligand were used as the "environment" during model building (20). The ligand-receptor contacts were coded for comparison (C01 to C14; Table 1).

Despite the low sequence identity between SIGLEC1 and PILRα (Fig. 5*A*), it is clear that most of the contacts are strikingly similar, even when the active site residues are not identical (Fig. 7, Table 1, and supplemental Fig. 7, *B* and *C*). First, the C03,

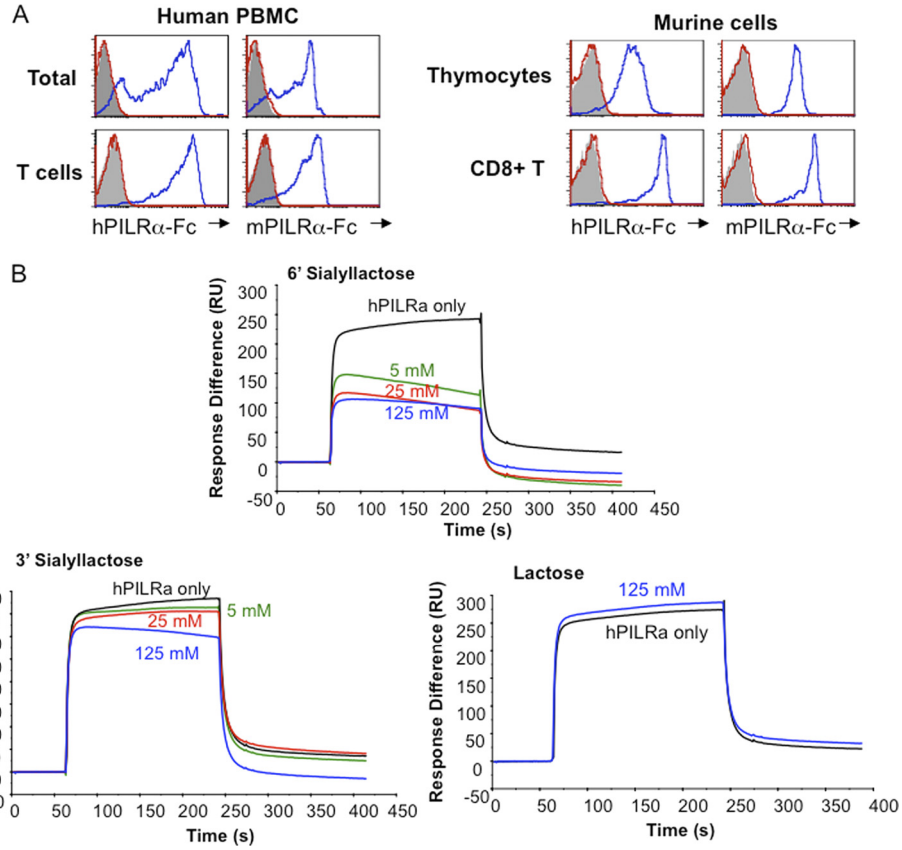

FIGURE 6. **Role of sialic acid in mediating PILRα/ligand interactions.** *A,* binding of hPILRα-Fc or mPILRα-Fc to sialidase A-treated (*red line*) and -untreated (*blue line*) total human PBMC and T cells (*left panels*) and mouse thymocyte and $CD8^+$ T cells (*right panels*) is shown, and the binding of isotype control to these cells is shown in *gray*. *B,* binding of hPILRα and the glycans to human NPDC1 was determined by SPR. Human NPDC1 (15 μg/ml) was immobilized to a CM5 sensor chip resulting in 4866.7 response units for the 6′-sialyllactose figure and 3787.3 response units for the 3′-sialyllactose and lactose figures. Human PILRa (1 μM) was used as a positive control. Lactose was used as a negative control for the glycans. For the competition experiment, human PILRα was incubated with various concentrations of the glycans at room temperature for 30 min before running as analyte over the chip. Sialylated carbohydrates containing sialic acid (Neu5Ac) in α2–3 (3′-siallylactose) and α2–6 linkage (6′-siallylactose) were used. Human PILRa was run between each glycan concentration to account for surface variability. Sensograms were corrected for response difference between active and reference flow cell.

C04 contacts (SIGLEC1.R197 *versus* PILRα.R126) and the C10 contact (SIGLEC1.W106 *versus* PILRα.W139) are identical. SIGLEC1.S103 and PILRα.T131 both accept a hydrogen bond via their backbone carboxylate oxygens from the ligand sialic acid O4 (contact C05). The backbone carboxylate oxygen of SIGLEC1.R105 and that of PILRα.Q138 accept a hydrogen bond from N5 of the ligand sialic acid (contact C08). For contact C09, the guanidine nitrogen of this arginine in SIGLEC1 interacts with the carboxylate of ligand sialic acid O1A (4.1 Å), although the side chain amino in the corresponding residue (PILRα.Q138) has the same contact, only slightly weaker (4.7Å). The peptidic backbone of SIGLEC1.L107 and the corresponding PILRα.Q140 have identical contacts with the ligand; their amino group contacts the ligand sialic acid O8 (coded as C11), and their carboxylate oxygen can accept a hydrogen bond from the ligand sialic acid O9 (coded as C12). Similarly, although SIGLEC1.W2 has proton/P_i interaction with the ligand sialic acid C11 with a distance of 3.6 Å, the base conformation of the corresponding residue (PILRα.Y33) is slightly further (5.4 Å), but a 30° rotation of the tyrosine side chain along CA-CB makes perfect overlay of the two aromatic systems, suggesting that the two receptors might have nearly identical contacts at this site too (C01).

Nonetheless, there are distinctive features that may explain the different binding profiles of ligands to SIGLEC1 *versus* PILRα. For example, the hydroxyl group of tyrosine 44 of SIGLEC1 donates a hydrogen bond to O6 of the ligand galactose (contact code C02). The corresponding residue in PILRα (Arg-74) faces away from the ligand, toward Phe-124. Instead, in PILRα the Gln-140 resides in this area. To explain the difference in binding of 3′-siallylactose *versus* 6′-siallylactose to PILRα (Fig. 6*B*), the structure of 6′-siallylactose was aligned to the fixed crystal conformation of 3′-siallylactose inside the active site of SIGLEC1/PILRα using the Flexible alignment application of MOE2011.10 with default settings (supplemental Fig. S8). The result suggests that the sialyl and glucosyl parts of the two ligands may align perfectly, despite the re-orientation of the galactoxyl group. In the context of the receptors, the rearrangement of the galactosyl in 6′-siallylactose brings all three hydroxyl groups (2′,3′,4′) toward the highly polar area of the cavity near Arg-126 and Gln-140 (PILRα).

In light of the experimental binding data, this suggests that the interaction of 3′-siallylactose with Arg-74 is not strong enough to out-compete the desolvation energy, so this compound lacks binding to PILRα. However, the additional polarity of 6′-siallylactose in

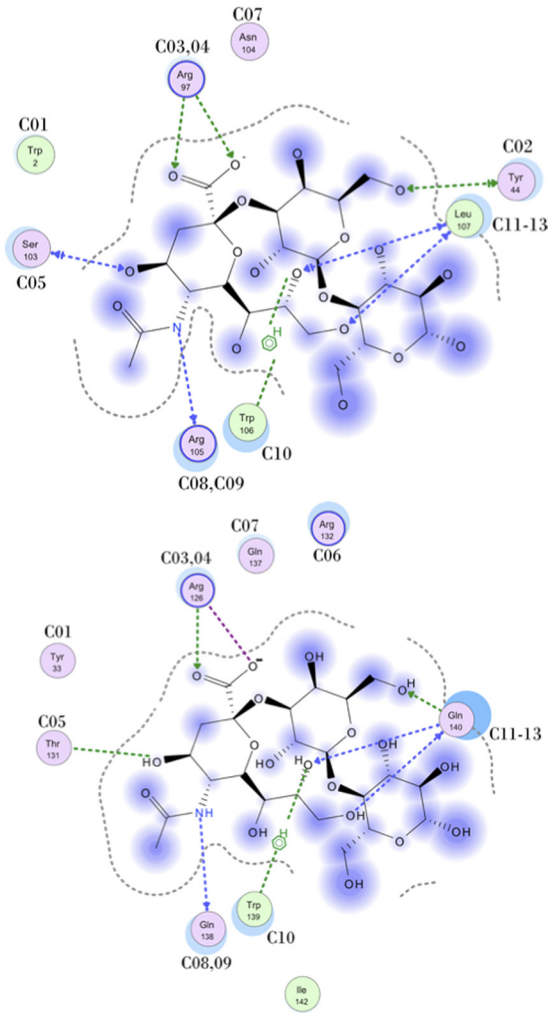

FIGURE 7. **Model of PILRα/ligand interactions based on SIGLEC1 structure.** Ligand interaction diagrams of SIGLEC1 (*top,* from Protein Data Bank structure 1QFO) and PILRα (*bottom,* from the homology model). Ligand contacts are numbered in *bold*, according to Table 1. Residues having hydrophobic contacts with the ligand are shown in *green*, and those having a polar or hydrogen bonding interactions are shown in *purple*. *Blue shading* denotes solvent-exposed atoms.

this region via the three galactosyl hydroxyls compensates the desolvation, hence the observable binding of 6′-siallylactose to PILRα. In summary, the active site of PILRα is very similar to that of SIGLEC1, with the exception that it is much more polar in the area that interacts with the galactoxyl group of the ligand.

DISCUSSION

Evolutionary Conservation of PILRα Ligand-interacting Domain—Our studies provide mechanistic insights into the interaction of PILRα and its ligands. We find that both human and mouse PILRα proteins cross-react with ligands from both human and mouse as well as primary cells from both species. This suggests that the ligand interaction domain of PILRα has been conserved through evolution. Correspondingly, the alignment of PILRα sequences points to a high degree of conservation among potential contact residues (Fig. 5*A*), some of which (Arg-126 and Trp-139) are shared with the SIGLEC family of receptors (12). Our studies demonstrate that one common binding mechanism involves the recognition of one or several sialic acid modifications in all ligands by the arginine conserved in mouse and human PILRα. We have come to this conclusion by showing that ligand fusion proteins, including mCD99-Fc, hNPDC1-Fc, and hCOLEC12-His, do not bind to hPILRαR126A and mPILRαR133A expressed on cell surfaces, whereas they all bind to WT human or mouse PILRα (Fig. 5*B*). Mutated fusion proteins hPILRαR126A-Fc and mPILRαR133A-Fc do not bind cell surface mCD99, hNPDC1, hCOLEC12, and HSV-1 gB (Fig. 5, *C* and *D*). Our SPR analysis shows that only WT hPILRα-Fc but not mutated hPILRαR126A-Fc is capable of ligand binding (Fig. 5*E*). Finally, hPILRαR126A-Fc and mPILRαR133A-Fc fail to interact with natural ligand(s) expressed on primary hematopoietic cells (Fig. 5*F*), suggesting this conserved arginine is required for binding to ligands in a more natural context. The uniform binding interaction mode of PILRα by sialic acid recognition might have evolved to trigger a conserved signaling pathway and functional outcome depending on which ligand(s) are encountered by PILRα. The convergence of PILRα sequences across different species may be indicative of receptor genes that are responding to evolutionary pressure provided by pathogens or unknown ligands (16).

TABLE 1

Ligand contacts of SIGLEC1 and the PILRα model

Ligand atoms are according to crystal structure (20). Some corresponding atomic distances are shown under comments for SIGLEC1 and PILRα.

	SIGLEC1		PILRα		
Contact code	Active site residue/atom	Ligand residue/atom	Active site residue/atom	Ligand residue/atom	Comments
C01	Trp-2.Ring	SIA201.C11	Tyr-33.Ring	SIA201.C11	3.6 *versus* 5.4 Å
C02	Tyr-44.OH	GAL202.O6	Arg-74.NH1/NH_2	GAL202.O6	[a]
C03	Arg-97.NH1	SIA201.O1A	Arg-126.NH1	SIA201.O1A	Identical
C04	Arg-97.NH_2	SIA201.O1B	Arg-126.NH_2	SIA201.O1B	Identical
C05	Ser-103.O	SIA201.O4	Thr-131	SIA201.O4	2.8 *versus* 4.8 Å
C06			Arg-132		[b]
C07	Asn-104.CA	SIA201.O4	Gln-137.OE1	SIA201.N5	5 *versus* 4.4 Å
C08	Arg-105.O	SIA201.N5	Gln–138.O	SIA201.N5	Identical
C09	Arg-105.NE	SIA201.O1A	Gln-138	SIA201.O1A	Identical
C10	Trp-106.Ring	SIA201.C9	Trp-139.Ring	SIA201.C9	Identical
C11	Leu-107.O	SIA201.O9	Gln-140.O	SIA201.O9	Identical
C12	Leu-107.N	SIA201.O8	Gln-140.N	SIA201.O8	[a]
C13	Leu-107.CD2	GAL202.O6	Gln140.NE2	GAL202.O6	3.8 *versus* 2.8 Å
C14	Asp-108		Ser-141		[c]

[a] Arg-74 in PILRα is facing away from the ligand, and making a hydrogen bond with Phe-124. However, this area is mostly occupied by Gln-140 in PILRα.
[b] Solvent-exposed side chain is indicated.
[c] Both residues are about 5 Å away from SIA201.O9.

Similarities between PILRα and SIGLECs—A highly conserved and essential arginine residue (Arg-197 in SIGLEC1) contacts the carboxylate group of sialic acid and two tryptophans that interact with the *N*-acetyl and glycerol moieties of *N*-acetylneuraminic acid (20, 21). Our functional data with arginine-mutated PILRα is consistent with a model in which SIGLECs and PILRα share some aspects of the ligand binding mechanisms. Our analysis identifies Arg-126 as a key contact residue in hPILRα (Arg-133 in mPILRα), and its location appears to be critical to mediate PILRα interaction with sialic acid on gB as well as other ligands. Further support of this model is provided by recent data showing the Trp-139 residue is also critical for human PILRα binding to HSV-1 gB (16). This Trp-139 is not present in PILRβ. Interestingly, the mutation of L139W in PILRβ does not confer the ability to mediate binding to HSV-1 gB, suggesting that there are other amino acids that specify PILRα/gB interactions (16). Based on a published structure of a SIGLEC1 coupled to sialic acid (20), it is possible to speculate on how PILRα might recognize sialic acid-containing ligands. The PILRα homology model identifies key active site residues that are shared with SIGLECs. Even in cases where residues were not identical, they were highly similar, strengthening our confidence in this model. Structural resolution of PILRα in the context of sialylated proteins will be necessary to define the precise interaction domains. Our preliminary competition binding studies and structural modeling show that PILRα preferentially binds to α2–6 over α2–3 sialic acid linkages. Additional studies are needed to extend such analysis against a variety of glycans structures. SIGLEC1 and multiple CD33-related SIGLECs can interact with sialic acids on pathogens such as *Neisseria meningitidis*, *Campylobacter jejuni*, group B *Streptococcus*, and *Trypanosoma cruzi* (19). An open question is whether PILRα can likewise interact directly with similar pathogens, which are known to carry sialylated sugar modifications on their surfaces. Our data and data from others (16) show that conserved residues in PILRα bind to ligands with sialic acid determinants. Although this intriguing similarity exists between SIGLECs and PILRα, several distinguishing features should be incorporated into the model of PILRα/ligand interactions. First, although both PILRa and SIGLECs can recognize sialic acid directly, PILRα does not show significant binding to selected glycan probes or to a glycan library, and 6′-sialylactose selectively but only partially (~50%) competes in ligand binding (12). Second, the residues shared by PILRα and SIGLECs are also found in PILRβ. However, PILRβ either does not bind to the ligands or it has much lower affinity, suggesting that the presence of the critical contact sites such as arginine and tryptophan are not sufficient to mediate binding (12, 16). Third, PILRα/ligand interactions have higher affinities (ranging from 0.049 to 1.1 μM for NPDC1 or COLEC-12, respectively, and 2.2 μM for mCD99 (12)) when compared with SIGLECs or other lectins that recognize glycans directly (19). Finally, our structural modeling suggests that several contact residues are exposed to solvent, which could serve as contact sites for amino acids within the ligands. Therefore, PILRα likely binds to a structural domain involving both sialic acid and protein determinants.

Complexity of PILRα/Ligand Interactions—It has been shown that mCD99, HSV-1 glycoprotein B, and PANP are PILRα ligands (6, 12, 15). Here, we find that human NPDC1 (K_D = 49 nM) and COLEC12 (K_D = 1.1 μM) can also recognize PILRα. NPDC1 has been identified as a neuron-specific gene involved in the control of cell proliferation and differentiation (31). Although the biological significance of these interactions is unknown, it appears that PILRα recognizes diverse ligands. The identification of multiple neuron-specific PILRα ligands (PANP and NPDC1) suggests PILRα might play a role in the central nervous system.

COLEC12 is the only member of the Collectin scavenger receptor family that is expressed as a cell surface transmembrane protein, and its ECD contains coiled-coil, collagen-like, and C-type lectin/carbohydrate domains (32). COLEC12 is expressed in vascular endothelial cells and monocytes and mediates the uptake of oxidized low density lipoproteins and microbes (32, 33). Interestingly, Collectins have been shown to interact with other inhibitory receptors such as signal regulatory protein α to modulate lung pathophysiology (41). Although the biology of PILRα and its interacting partners COLEC12 and NPDC1 is not understood, PILRα is emerging as a receptor that recognizes a group of ligands bearing a unique sialic acid signature. Correspondingly, we found that human and mouse PILRα-Fc fusions bind to mouse thymocytes, peripheral $CD8^+$ T cells, as well as a majority of human PBMCs and especially T cells. These data suggest that PILRα ligands are broadly expressed in immune cells, and multiple ligands might contribute to the binding of certain cell types to PILRα. Because the presence of sialylated glycan is a common feature of all known PILRα ligands, we would predict that PILRα might have additional unknown cellular ligands.

Conclusions—An evolutionarily conserved domain containing an arginine residue (hPILRαR126 and mPILRαR133) is required for PILRα interaction with multiple sialylated ligands, including two newly identified ligands, NPDC1 and COLEC12. Despite a striking similarity between the PILRα and the SIGLEC binding pocket, PILRα appears to recognize both sialic acid and a protein domain on ligands. The PILRα interactions involve different ligands with varied affinities and anatomic locales. Challenges for the future are to understand how these ligands are important in mediating the biological functions of PILRα, to elucidate the role of sialic acid and protein determinants in PILRα biology, and to dissect the signaling pathways that are triggered upon ligand interaction.

Acknowledgments—We are grateful to Drs. Flavius Martin, John Lowe, Harinder Singh, Eric Brown, Menno van Lookeren Campagane, and Dan Eaton for providing insightful discussions. We thank Michelle Irwin, Leslie Welch, and Louisette Basa for helping with LC-MS analysis.

REFERENCES

1. Daëron, M., Jaeger, S., Du Pasquier, L., and Vivier, E. (2008) Immunoreceptor tyrosine-based inhibition motifs. A quest in the past and future. *Immunol. Rev.* **224,** 11–43
2. Taylor, L. S., Paul, S. P., and McVicar, D. W. (2000) Paired inhibitory and activating receptor signals. *Rev. Immunogenet.* **2,** 204–219
3. Ravetch, J. V., and Lanier, L. L. (2000) Immune inhibitory receptors. *Science* **290,** 84–89
4. Fournier, N., Chalus, L., Durand, I., Garcia, E., Pin, J. J., Churakova, T., Patel, S., Zlot, C., Gorman, D., Zurawski, S., Abrams, J., Bates, E. E., and

Garrone, P. (2000) FDF03, a novel inhibitory receptor of the immunoglobulin superfamily, is expressed by human dendritic and myeloid cells. *J. Immunol.* **165,** 1197–1209
5. Mousseau, D. D., Banville, D., L'Abbé, D., Bouchard, P., and Shen, S. H. (2000) PILRα, a novel immunoreceptor tyrosine-based inhibitory motif-bearing protein, recruits SHP-1 upon tyrosine phosphorylation and is paired with the truncated counterpart PILRβ. *J. Biol. Chem.* **275,** 4467–4474
6. Shiratori, I., Ogasawara, K., Saito, T., Lanier, L. L., and Arase, H. (2004) Activation of natural killer cells and dendritic cells upon recognition of a novel CD99-like ligand by paired immunoglobulin-like type 2 receptor. *J. Exp. Med.* **199,** 525–533
7. Banerjee, A., Stevenaert, F., Pande, K., Haghjoo, E., Antonenko, S., Gorman, D. M., Sathe, M., McClanahan, T. K., Pierce, R., Turner, S. P., Bigler, M. E., Phillips, J. H., and Heyworth, P. G. (2010) Modulation of paired immunoglobulin-like type 2 receptor signaling alters the host response to *Staphylococcus aureus*-induced pneumonia. *Infect. Immun.* **78,** 1353–1363
8. Kogure, A., Shiratori, I., Wang, J., Lanier, L. L., and Arase, H. (2011) PANP is a novel *O*-glycosylated PILRα ligand expressed in neural tissues. *Biochem. Biophys. Res. Commun.* **405,** 428–433
9. Satoh, T., Arii, J., Suenaga, T., Wang, J., Kogure, A., Uehori, J., Arase, N., Shiratori, I., Tanaka, S., Kawaguchi, Y., Spear, P. G., Lanier, L. L., and Arase, H. (2008) PILRα is a herpes simplex virus-1 entry coreceptor that associates with glycoprotein B. *Cell* **132,** 935–944
10. Schenkel, A. R., Mamdouh, Z., Chen, X., Liebman, R. M., and Muller, W. A. (2002) CD99 plays a major role in the migration of monocytes through endothelial junctions. *Nat. Immunol.* **3,** 143–150
11. Wingett, D., Forcier, K., and Nielson, C. P. (1999) A role for CD99 in T cell activation. *Cell. Immunol.* **193,** 17–23
12. Tabata, S., Kuroki, K., Wang, J., Kajikawa, M., Shiratori, I., Kohda, D., Arase, H., and Maenaka, K. (2008) Biophysical characterization of *O*-glycosylated CD99 recognition by paired Ig-like type 2 receptors. *J. Biol. Chem.* **283,** 8893–8901
13. Wang, J., Shiratori, I., Satoh, T., Lanier, L. L., and Arase, H. (2008) An essential role of sialylated *O*-linked sugar chains in the recognition of mouse CD99 by paired Ig-like type 2 receptor (PILR). *J. Immunol.* **180,** 1686–1693
14. Kelm, S., and Schauer, R. (1997) Sialic acids in molecular and cellular interactions. *Int. Rev. Cytol.* **175,** 137–240
15. Satoh, T., and Arase, H. (2008) HSV-1 infection through inhibitory receptor, PILRα. *Uirusu* **58,** 27–36
16. Fan, Q., and Longnecker, R. (2010) The Ig-like v-type domain of paired Ig-like type 2 receptor α is critical for herpes simplex virus type 1-mediated membrane fusion. *J. Virol.* **84,** 8664–8672
17. Wang, J., Fan, Q., Satoh, T., Arii, J., Lanier, L. L., Spear, P. G., Kawaguchi, Y., and Arase, H. (2009) Binding of herpes simplex virus glycoprotein B (gB) to paired immunoglobulin-like type 2 receptor α depends on specific sialylated *O*-linked glycans on gB. *J. Virol.* **83,** 13042–13045
18. Fan, Q., Lin, E., Satoh, T., Arase, H., and Spear, P. G. (2009) Differential effects on cell fusion activity of mutations in herpes simplex virus 1 glycoprotein B (gB) dependent on whether a gD receptor or a gB receptor is overexpressed. *J. Virol.* **83,** 7384–7390
19. Crocker, P. R., Paulson, J. C., and Varki, A. (2007) Siglecs and their roles in the immune system. *Nat. Rev. Immunol.* **7,** 255–266
20. May, A. P., Robinson, R. C., Vinson, M., Crocker, P. R., and Jones, E. Y. (1998) Crystal structure of the N-terminal domain of sialoadhesin in complex with 3′-sialyllactose at 1.85-Å resolution. *Mol. Cell* **1,** 719–728
21. Munday, J., Floyd, H., and Crocker, P. R. (1999) Sialic acid binding receptors (siglecs) expressed by macrophages. *J. Leukocyte Biol.* **66,** 705–711
22. Wilson, M. D., Cheung, J., Martindale, D. W., Scherer, S. W., and Koop, B. F. (2006) Comparative analysis of the paired immunoglobulin-like receptor (PILR) locus in six mammalian genomes. Duplication, conversion, and the birth of new genes. *Physiol. Genomics* **27,** 201–218
23. Gonzalez, L. C., Loyet, K. M., Calemine-Fenaux, J., Chauhan, V., Wranik, B., Ouyang, W., and Eaton, D. L. (2005) A coreceptor interaction between the CD28 and TNF receptor family members B and T lymphocyte attenuator and herpesvirus entry mediator. *Proc. Natl. Acad. Sci. U.S.A.* **102,** 1116–1121
24. Shields, R. L., Namenuk, A. K., Hong, K., Meng, Y. G., Rae, J., Briggs, J., Xie, D., Lai, J., Stadlen, A., Li, B., Fox, J. A., and Presta, L. G. (2001) High resolution mapping of the binding site on human IgG1 for FcγRI, FcγRII, FcγRIII, and FcRn and design of IgG1 variants with improved binding to the Fcγ R. *J. Biol. Chem.* **276,** 6591–6604
25. Keck, R. G., Briggs, J. B., and Jones, A. J. (2005) Oligosaccharide release and MALDI-TOF MS analysis of *N*-linked carbohydrate structures from glycoproteins. *Methods Mol. Biol.* **308,** 381–396
26. Anumula, K. R., and Taylor, P. B. (1992) A comprehensive procedure for preparation of partially methylated alditol acetates from glycoprotein carbohydrates. *Anal. Biochem.* **203,** 101–108
27. Cooper, C. A., Gasteiger, E., and Packer, N. H. (2001) GlycoMod. A software tool for determining glycosylation compositions from mass spectrometric data. *Proteomics* **1,** 340–349
28. Munson, P. J., and Rodbard, D. (1980) Ligand. A versatile computerized approach for characterization of ligand-binding systems. *Anal. Biochem.* **107,** 220–239
29. Molecular Operating Environment (2011) 1010 Sherbooke St. West, Suite 910, Montreal, Quebec H3A 2R7, Canada
30. Clark, A. M., and Labute, P. (2007) Two-dimensional depiction of protein-ligand complexes. *J. Chem. Inf. Model.* **47,** 1933–1944
31. Galiana, E., Vernier, P., Dupont, E., Evrard, C., and Rouget, P. (1995) Identification of a neuron-specific cDNA, NPDC-1, able to down-regulate cell proliferation and to suppress transformation. *Proc. Natl. Acad. Sci. U.S.A.* **92,** 1560–1564
32. Ohtani, K., Suzuki, Y., Eda, S., Kawai, T., Kase, T., Keshi, H., Sakai, Y., Fukuoh, A., Sakamoto, T., Itabe, H., Suzutani, T., Ogasawara, M., Yoshida, I., and Wakamiya, N. (2001) The membrane-type collectin CL-P1 is a scavenger receptor on vascular endothelial cells. *J. Biol. Chem.* **276,** 44222–44228
33. Nakamura, K., Funakoshi, H., Miyamoto, K., Tokunaga, F., and Nakamura, T. (2001) Molecular cloning and functional characterization of a human scavenger receptor with C-type lectin (SRCL), a novel member of a scavenger receptor family. *Biochem. Biophys. Res. Commun.* **280,** 1028–1035
34. Julenius, K., Mølgaard, A., Gupta, R., and Brunak, S. (2005) Prediction, conservation analysis, and structural characterization of mammalian mucin-type *O*-glycosylation sites. *Glycobiology* **15,** 153–164
35. Gelin, C., Aubrit, F., Phalipon, A., Raynal, B., Cole, S., Kaczorek, M., and Bernard, A. (1989) The E2 antigen, a 32-kDa glycoprotein involved in T-cell adhesion processes, is the MIC2 gene product. *EMBO J.* **8,** 3253–3259
36. North, S. J., Huang, H. H., Sundaram, S., Jang-Lee, J., Etienne, A. T., Trollope, A., Chalabi, S., Dell, A., Stanley, P., and Haslam, S. M. (2010) Glycomics profiling of Chinese hamster ovary cell glycosylation mutants reveals *N*-glycans of a novel size and complexity. *J. Biol. Chem.* **285,** 5759–5775
37. Olson, F. J., Bäckström, M., Karlsson, H., Burchell, J., and Hansson, G. C. (2005) A MUC1 tandem repeat reporter protein produced in CHO-K1 cells has sialylated core 1 *O*-glycans and becomes more densely glycosylated if coexpressed with polypeptide-GalNAc-T4 transferase. *Glycobiology* **15,** 177–191
38. Masuda, K., Yamaguchi, Y., Kato, K., Kim, H. H., Takahashi, N., Shimada, I., and Arata, Y. (1999) Post-translational modifications of immunoglobulin G. A mouse IgG variant that lacks the entire CH1 domain. *Mol. Immunol.* **36,** 993–1003
39. Ikehara, Y., Ikehara, S. K., and Paulson, J. C. (2004) Negative regulation of T cell receptor signaling by Siglec-7 (p70/AIRM) and Siglec-9. *J. Biol. Chem.* **279,** 43117–43125
40. Vinson, M., van der Merwe, P. A., Kelm, S., May, A., Jones, E. Y., and Crocker, P. R. (1996) Characterization of the sialic acid-binding site in sialoadhesin by site-directed mutagenesis. *J. Biol. Chem.* **271,** 9267–9272
41. Janssen, W. J., McPhillips, K. A., Dickinson, M. G., Linderman, D. J., Morimoto, K., Xiao, Y. Q., Oldham, K. M., Vandivier, R. W., Henson, P. M., and Gardai, S. J. (2008) Surfactant proteins A and D suppress alveolar macrophage phagocytosis via interaction with SIRPα. *Am. J. Respir. Crit. Care Med.* **178,** 158–167